Solid-state ^{13}C NMR spectroscopy — A powerful characterization tool for thermotropic liquid crystals

T. Narasimhaswamy

Abstract | Thermotropic liquid crystals are quintessential materials. The self organization of them at molecular level leads to orientational order, an important property both for academic and industrial interest. Additionally, their sensitivity to external stimuli like temperature, pressure, mechanical, electrical, magnetic field etc. make them as natural choice for smart advanced materials. The contemporary molecular designing of mesogens has undergone dramatic change and accordingly different molecular topologies are being explored for inducing the novel mesophases and morphologies. The understanding of their interactions at molecular level is very crucial in designing future advanced materials for challenging applications. To address these challenges, understanding of current mesogenic molecular structures and their organization at different levels is utmost important. This article focuses on the role of solid state ^{13}C NMR as a characterization tool for molecular level understanding of mesogens. As the ^{13}C NMR spectroscopy in mesophase is marred by anisotropic interactions, it differs from conventional solution technique. Hence, this article is aimed at explaining the role of anisotropic interactions that influence the ^{13}C chemical shifts and ^{13}C-^{1}H dipolar couplings of a mesogen in liquid crystalline phase. A brief historical development of ^{13}C NMR (1D) and separated local field spectroscopy (2D) is presented and their role for deducing the important information in the mesophase is highlighted. The relevant subtleties like alignment induced chemical shifts and ^{13}C-^{1}H dipolar couplings for range of calamitic mesogens is shown while the work on other molecular shapes are cited based on their significance. Finally, the future role of ^{13}C NMR spectroscopy for understanding complex mesogens is briefly mentioned.

Thermotropic liquid crystals

Matter exists in nature in three forms – (i) solid (ii) liquid and (iii) gas [1]. The molecules comprised of matter would differ in their arrangement leading to the formation of thermodynamically identifiable phases — solid, liquid and gases. The crystalline solid macroscopically viewed, posses shape and volume while liquids have volume but adopt the shape of the container whereas gas fills the entire volume of the container [2]. At molecular level, the crystalline solid possess long-range positional and orientational order while liquids have no order due to molecular tumbling. Similarly gases too do not have order and also the intermolecular distances are

Polymer Lab, Central Leather Research Institute, Adyar, Chennai 600 020

Figure 1: Anatomy of a thermotropic liquid crystal (calamitic mesogen).

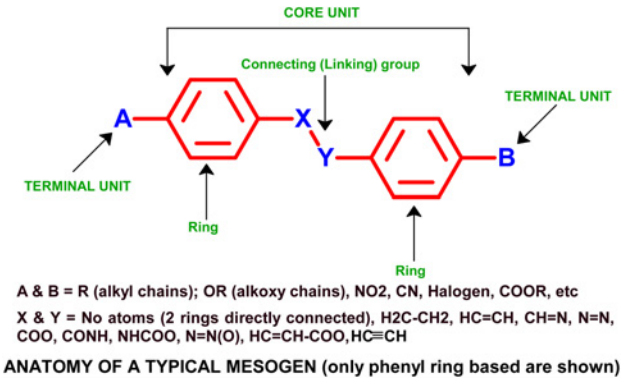

very high [3]. However, a class of molecules (mostly organic) exhibits yet another phase popularly known as Fourth State of Matter [4]. Molecules in this phase possess positional/orientational order and also exhibit flow. Macroscopically they appear like opaque fluids. Molecules exhibiting this phase are classified as Thermotropic Liquid Crystals as variation in temperature brings the change [5]. For instance, material exhibiting thermotropic liquid crystalline phase when cooled crystallizes to solid and heating leads to isotropic liquid. As a result, these phases are also known as mesophases since liquid crystal phase is noticed between crystalline solid and isotropic liquid. Subsequently, molecules exhibiting mesophases are termed as mesogens [6].

Historically, Friedrick Reinitzer, an Austrian Botanist observed liquid crystal phenomena in 1888 for cholesterol benzoate [7]. This material when heated showed a transition at 145.5°C to opaque fluid which upon further heating transformed to transparent isotropic liquid at 178.5°C. Later many researchers have undertaken investigation on these interesting molecules and established the structure-property relationship [8]. These studies provided a basis for designing a new mesogen and accordingly the anatomy of liquid crystals is established [9] (Figure 1). The research focus till 1960's is on synthesis and property studies of mesogens while the first application of liquid crystals is witnessed in 1970's as a display material for wrist watches [10].

Thermotropic liquid crystals are broadly classified into (i) Calamitic and (ii) Discotic [11] (Figure 2). The former denotes rod-like and later represents disc-like molecular shape. However, developments in recent past had lead to variety of molecular shapes as building blocks for liquid crystalline materials [12]. The spurt in liquid crystal research both by the academia and industry is attributed to their success as display materials in the current opto-electronic devices [13]. For instance, their mature developments as displays in flat-panel and high-definition TV screens, mobile devices, palm computers, thermo chromic sensors, optical shutters and many other advanced applications has prompted multi-national companies to invest in their R&D centers. Consequently, the liquid crystals are currently classified as advanced materials and many research groups are globally concentrating on new developments [14]. The academic spurt on these advanced materials is marked initially by the discovery of discotic & columnar liquid crystals and later banana mesogens [15]. These two important developments largely lead to current scenario which typifies true interdisciplinary activity encompassing many research specializations. More particularly developments witnessed after 1990's had paved the way for novel designing approaches for thermotropic liquid crystals. This dramatic change resulted in paradigm shift in molecular designing of mesogens. For instance, the conventional design primarily relies on parameters like geometrical anisotropy, linearity and anisotropic polarisability [16] the current approach emphasizes on molecular shape and topology, reduced symmetry, microphase segregation, self-assembly and self-organization etc [17]. This novel approach has resulted in to a large variety of mesophase morphologies like lamellar, cubic, columnar, bicontinous 3D phases etc [18]. As a consequence, new models are proposed to understand and explain the appearance of complex mesophase morphologies. Among them, model based on micro/nano-phase segregation of different parts of the mesogens driven by non-covalent interactions has attained popularity [19].

Figure 2: Broad classification of thermotropic liquid crystals.

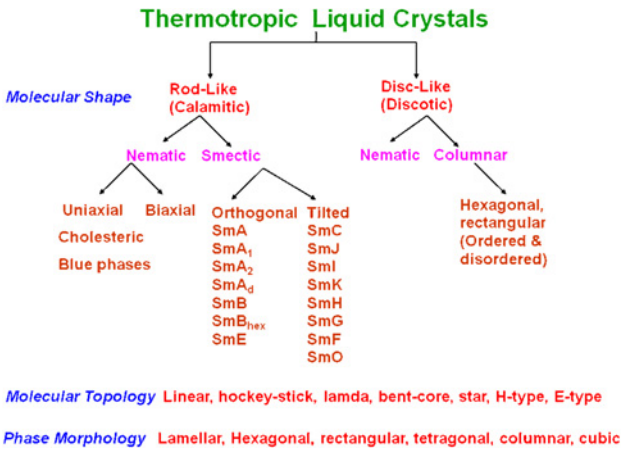

In this model the mesogen is considered as shape anisometric (anisotropy) unit and different parts of the molecules are governed by variety of interactions like dipole-induced dipole, ionic, charge-transfer, π-stacking and hydrogen bonding [20]. In this approach, the mesogen is also treated as block of rigid and soft segments which in mesophase experience different dynamics.

Characterization tools

The understanding of mesogens at molecular level is of paramount importance not only for establishing property-structure correlations but also designing future materials for advanced applications. The characterization of them in the mesophase is a rational way of understanding the issues like role of molecular topology and packing, nano-segregation, non-covalent interactions, orientation order, dynamics of different segments etc. As mentioned earlier, shape anisotropy (anisometry) is one of the important designing parameter of liquid crystals [21]. Anisotropy (Anisometry) is a property of material which changes with directions in a three dimensional space. The molecular shape anisotropy in turn induces other properties like anisotropic flow, optical & chemical shift anisotropy, anisotropic magnetic susceptibility and dielectric polarisability etc. in liquid crystals [22]. If the measurements are carried out in the mesophase, these properties can be suitably investigated employing various tools. For instance, optical polarizing microscopy provides optical anisotropy (birefringence) [23], NMR gives chemical shift anisotropy [24], dielectric spectroscopy measures dielectric anisotopric polarisability [25] etc. In other words, measurements carried out in the mesophase are source of wealth of information while similar measurements either in isotropic phase or solution are devoid off. As a result, studies pertaining to anisotropic properties in the mesophase are increasingly gaining importance [26]. The usual way of characterizing mesogens is to identify the phase by optical poarising microscopy, establish the thermodynamic reversibility using differential scanning calorimetry and deduce molecular arrangements using powder X-ray diffraction [27]. The other spectroscopic tools like FT-IR [28], FT-Raman spectroscopy [29] and refractive index [30] measurements are also undertaken to find mainly the changes in the phase and orientational order. The solution NMR spectroscopy, on the other hand, is routinely used for structural characterization of mesogens in isotropic phase [31]. However, in the past decade solid-state NMR has emerged as powerful tool for molecular structural characterization of liquid crystals in the mesophase [32].

NMR of thermotropic liquid crystals

Saupe and Englert are the first to investigate the dissolved molecules (benzene) in liquid crystal using the ^{1}H NMR spectroscopy [33]. As the signals are broadened by ^{1}H-^{1}H homo-nuclear dipolar interactions, second moment analysis is used for extracting structural details. Prior to them, the liquid crystalline NMR consisted of broad features (low resolution) [34]. Later many researchers have used deuterium NMR for probing the molecular dynamics and orientational order in liquid crystals [35]. The quadrupole interactions which are sensitive to molecular dynamics are typically used for investigations [36]. However, deuterium NMR demands labeling of the liquid crystalline molecules which necessitate the use of labeled samples in the synthesis. For structurally simple mesogens, the labeling can be done with ease. On the other hand, for liquid crystals with complex molecular structures, labeling demand extra efforts from synthetic chemists. Additionally, complete labeling of the sample with deuterium would result in broad lines due to quadrupolar interactions. Hence, selectively labeled samples are used for deuterium NMR investigations. In the case of natural abundance ^{13}C NMR, the labeling is not needed and the synthesized mesogen can be subjected to investigation. Moreover, each resolved signal would be a source of information thus providing greater opportunity to probe every segment of the molecule. In view of these specific advantages, the ^{13}C NMR spectroscopy has emerged as a powerful tool for probing mesogens in liquid crystalline phase [37]. With the advent of 2D separated local field spectroscopy, the ^{13}C NMR has attained special status for probing liquid crystals as indicated by recent literature [38]. Hence in the present review focus is placed on the utility of solid state ^{13}C NMR spectroscopy for structural characterization of mesogen in liquid crystalline phases and explores the possible role it would play in future advancement of the field.

^{13}C NMR spectroscopy in mesophase

The ^{13}C NMR (solution) is routinely used for structure determination/identification of organic molecules as mentioned earlier [31]. The chemical shift is backbone of NMR spectroscopy. It is an anisotropic property and is described by a tensor (3×3 matrix) with principal shielding components σ_{xx}, σ_{yy} and σ_{zz} [39]. In solution, the principal shielding components of the chemical shift tensor averages out due to fast molecular tumbling resulting in isotropic chemical shift (σ_{iso}). However, in solid state and liquid crystalline state, due to anisotropic nature of phase, the

Figure 3: CSA Tensor and symmetry of the group.

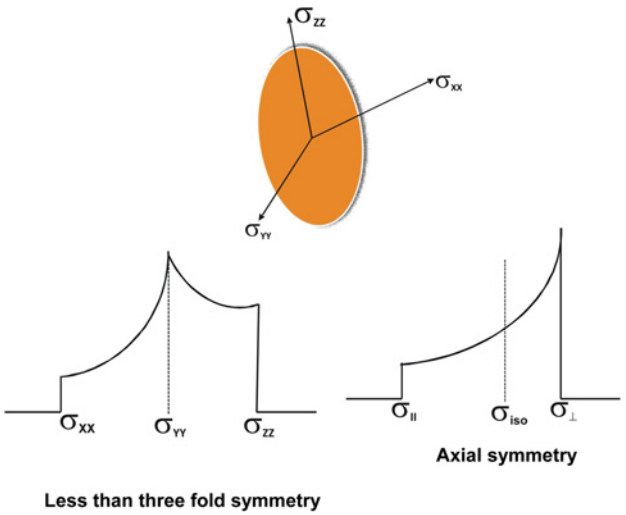

CSA manifests [40]. As a result, the chemical shift values of mesogen are different in liquid crystalline phase in contrast to their solution NMR. Moreover, when a liquid crystalline sample is placed in magnetic field, the molecules depending upon the sign of the anisotropic magnetic susceptibility tensor can align parallel or perpendicular to the magnetic field [41]. For instance, mesogens with positive sign of susceptibility tensor would orient parallel to the field whereas those with negative sign prefer perpendicular orientation. This results in change of chemical shift as the CSA tensor orientation depends on the applied magnetic field and molecular orienting axis (molecular axis or long axis) [42]. Interestingly, the alignment induced shift (AIS) which is determined by subtracting the chemical shift values in the liquid crystalline phase and solution ($\delta_{lc} - \delta_{\text{iso}}$) provides important information about the orientation of the mesogen in the applied magnetic field [43]. The magnitude of the anisotropic chemical shifts in liquid crystalline state is governed by the orientation of the principal axes of the carbon site of the molecule with respect to the magnetic field. As a convention, the magnetic field axis is taken as Z axis in a laboratory frame. Considering the laboratory frame as reference frame, the orientation of principal axes of the chemical shift tensor which depends on the symmetry of the particular carbon site and molecular orienting axis, the chemical shift values are arrived [44]. In other words, site symmetry, molecular orientation in the magnetic field decides the final chemical shift value of carbons of a mesogen in liquid crystalline phase. For instance, in the case of $-CH_3$ group which is axially symmetric, the chemical shift anisotropy manifests in to $\sigma_{||}$ & $\sigma_{\perp}$. For those groups which are less than threefold symmetry, the pattern would be σ_{zz}, σ_{yy} and σ_{xx}[39] (Figure 3). In consequence, the assignment of carbon-13 peaks in the spectrum involves usage of CSA values and their orientation with respect to laboratory frame [44].

In addition to field induced orientation, the molecules undergo rapid rotations with respect to their long (molecular) axis in liquid crystalline phase. Consequently, the transformation of lab to molecular frame involving use of principal axes of the chemical shift tensor and Euler angles is needed to assign the chemical shift for different carbons of mesogen [44]. The CSA tensors of only few of the structural units that are employed for constructing the mesogens are reported in literature [45]. Moreover, the CSA pattern is very sensitive to local chemical environment, the use of literature values would eventually lead to errors in assigning chemical shifts in the mesophase. An ideal situation would be to determine the CSA pattern of the mesogen in the solid phase and use them for assigning the mesophase chemical shifts [46]. Such an approach would minimize the errors as the chemical environment of the sample both in solid and liquid crystalline phase would be similar. Variety of experiments are practiced in literature to determine the CSA pattern which include magic angle spinning (MAS) at different spinning speeds [47], magic angle turning (MAT) [48], DE TOSS [49] (total suppression of spinning side bands) and SUPER (separation of undistorted powder patterns by effortless recoupling) [50] experiments. In view of these practical problems, the precise assignment of chemical shifts of individual carbons of the mesogen in the liquid crystalline phase is difficult task. In literature, this assignment is carried out by comparing the structurally similar mesogens reported by other workers and by noticing the relative intensity of the signals [51]. Yet another way is to make use of chemical shift values of starting materials if they are mesogenic. For instance, 4-alkoxy benzoic acids are one of the well utilized starting materials for many liquid crystalline molecules. These are one (phenyl) ring based molecules and exhibit mesophases (both nematic and smectic) depending up on the alkoxy chain length due to intermolecular hydrogen bonding [52]. The mesophase chemical shifts of these molecules would ideally serve as reference for other mesogens which are made of them. For instance, 4-hexyloxy benzoic acid exhibits nematic phase ($T_{C-N} - 105.4°C$ and $T_{N-I} - 153.2°C$) and measuring ^{13}C NMR spectrum in the phase would serve as useful source for alkoxy benzoic acid based liquid crystals.

In the year 1974, Pines group first reported the ^{13}C NMR spectra of thermotropic liquid crystals in the mesophase [53]. In a series of papers, they demonstrated the high resolution spectra of MBBA and PAA using proton decoupled cross-polarization experiments [54, 55]. These variable temperature experiments thus provided structural information for the first time in the solid state, mesophase and isotropic liquid. The notable features of the study include the ^{13}C line broadening in solid state, resolution enhancement and variation of chemical shift with changes in temperature in mesophase and isotropic averaging of chemical shifts in the liquid state. Further, the downfield chemical shifts of aromatic and azomethine carbons and upfield shift for aliphatic chains (terminal groups) is explained based on the orientation of principal axes of chemical shift tensors. Additionally, the appearance of one line each for ortho and meta carbons is attributed to π-flips of phenyl rings. For $-OCH_3$ group, the small change in the chemical shift moving from isotropic to liquid crystalline phase is attributed to orientation of $-OCH_3$ axis closed to magic angle with respect to Director. By employing the chemical shift anisotropy values, the orientational order is calculated at different temperatures. In the case of MBBA one molecular order (S) is proposed based on the AIS values and an angle of θ (9°) between the para axis and molecular axis (molecular director) is assumed. The efficient cross polarization of ^1H to ^{13}C spins in liquid crystals is assigned to order fluctuations. They also extended similar approach to homologous series of p-alkoxy azoxy benzenes [56]. The molecular order variation with respect to odd-even effect is established using ^{13}C chemical shift in the mesophase. Since then, the ^{13}C NMR spectroscopy has become popular and many research groups have been using the technique for characterization of variety of liquid crystalline molecules [57].

Among other researchers, Fung and co workers have used ^{13}C NMR spectroscopy to study the structure and orientational order for variety of liquid crystals in mid 80's to 90's [58–60]. However, majority of their work focused on commercially available liquid crystals which are relatively simple in contrast to large body of synthesized mesogens. Later Dong et al. started employing ^{13}C NMR spectroscopy realizing the potentiality of the technique in probing every segment of mesogen [61]. After the discovery of discotic/columnar liquid crystals, the ^{13}C NMR spectroscopy is also extended to their study [62]. As synthetic groups engaged in liquid crystal research progressed with many novel complex mesogens and mesophases, the usage of ^{13}C NMR spectroscopy for their characterization also witnessed development [63]. Currently, ^{13}C NMR spectroscopy is used both as confirmative and complimentary evidence from deuterium NMR spectroscopy [64].

Separated local field spectroscopy

Separated Local Field spectroscopy (SLF) is a 2D solid state NMR technique which enables the separation of ^{13}C chemical shifts from ^{13}C-^1H dipolar couplings of solid (single crystals) or liquid crystals without use of magic angle spinning [65]. The resolution enhancement due to the separation of chemical shifts and dipolar couplings made this technique more powerful for structural characterization of liquid crystals. Usually ^{13}C NMR of a solid sample under normal condition yields broad featureless lines typical of wide line NMR [66]. The line broadening in solid state ^{13}C NMR is contributed by three factors — (i) dipolar broadening (ii) chemical shift anisotropy and (iii) low signal/noise ratio due to low natural abundance & gyromagentic ratio of ^{13}C nuclei [67]. The dipolar broadening arises due to the interaction of spins with their neighbors in a solid lattice. The dipolar broadening is also anisotropic property like CSA as discussed in the earlier section and depends on the orientation of molecule in the magnetic field. In isotropic solution (liquids) the dipolar broadening vanishes as molecules tumble freely. The dipolar broadening in the case of organic molecules is made up of ^1H–^1H (homo nuclear) and ^{13}C–^1H (hetero nuclear) dipolar interactions. The homo nuclear broadening is very high in magnitude ($\sim$ 100 kHz) in contrast to hetero nuclear broadening ($\sim$ 23 kHz) while the broadening arising from ^{13}C–^{13}C is insignificant due to their low natural abundance [68]. However, the broadening arising due to chemical shift anisotropy for oriented molecules like liquid crystals is less as they are orientationally ordered and also involve in rotational motions along the long axis. As a consequence, to get high resolution 2D ^{13}C NMR for liquid crystals, the dipolar broadening has to be manipulated. In other words, the broadening arising for liquid crystals in ^{13}C NMR is mainly from dipolar interactions and by efficient selective dipolar decoupling schemes, the spectral resolution can be enhanced. In SLF spectroscopy, homo nuclear dipolar broadening is selectively removed by applying suitable decoupling sequence while retaining ^{13}C–^1H dipolar couplings [69]. In order to enhance the sensitivity of ^{13}C (dilute spins), cross-polarisation is employed where transfer of ^1H spin magnetization to dilute ^{13}C spins is carried out using Hartman-Hahn match [70]. As a result, the SLF spectrum shows well resolved ^{13}C chemical shifts in f2 dimension and ^{13}C–^1H dipolar couplings in f1 dimension.

In the year 1976, Waugh's group first introduced separated local field spectroscopy [71]. To suppress the ^1H–^1H homo nuclear dipolar interactions, multiple pulse based WAHUHA pulse sequence

is used while ^{13}C sensitivity is enhanced by cross polarization. The utility of SLF is demonstrated on ^{13}C labeled calcium formate single crystal and later on oriented polyethylene [69,72]. However, the use of SLF for liquid crystals is reported by Ernst et al. in 1979 on MBBA [73]. The study included the deuterium coupled ^{13}C NMR, ^{15}N–^{13}C coupled ^{13}C NMR along with separated local field spectroscopy. The detailed investigations revealed the orientational constraints for MBBA in the mesophase. The important outcome of the work is that in arriving the orientational order, the angle (θ) between the para-axis of the phenyl ring and long axis is found to be 3.5° in contradiction to earlier literature values. These early studies demonstrated that the successful implementation of SLF spectroscopy depends on certain crucial parameters. They include selective and efficient decoupling sequence and the resulting scaling factor which would influence the overall resolution of the spectrum [74]. In other words, the efficient decoupling sequence usually results in sharp dipolar splitting with narrow line width. Further, the selection of the decoupling sequence also alters the splitting pattern of the dipolar slice. For instance, the –C–H carbon produces doublet in SLF experiment while the long range dipolar coupling between carbons and protons which are separated by more than one bond is also possible [75]. Then the additional splitting would serve as a source of information for understanding the mesophase structure. Another practical problem with SLF for liquid crystals is the heating up of the sample by high RF currents used for suppressing the dipolar decoupling [76]. The initial SLF schemes had some of these problems and many researchers attempted to address them to improve the spectral resolution without hampering the mesophase characteristics.

Fung et al. extensively used SLF spectroscopy for studying a large number of liquid crystals [77–81]. They proposed new approach which involves use of SLF in combination with Variable angle spinning (VAS). The scheme encompasses, slow spinning of the sample at other than magic angle and simultaneously running SLF sequence. The spinning of sample and low power decoupling had ensured the reduction of dipolar broadening while SLF provided high resolution leading to ^{13}C–^{1}H dipolar slices. In many cases long range couplings of the dipolar slices of core unit are clearly seen which are used for computing the orientational order. In spite of large success of VAS-SLF for probing large number of liquid crystals, the method had certain limitations. The spinning of the sample is essential feature of VAS-SLF and the angle is crucial parameter which not only affects the scaling factor but also influences dipolar resolution. Small errors in setting up the spinning angle would results in either loss of resolution or erroneous dipolar couplings.

Pines and coworkers, in 1996 introduced new pulse scheme named as Proton Detected Local Field Spectroscopy (PDLF) and applied on a nematogen, 4′-pentyl-4-biphenylcarbonitrile [82]. The ^{13}C-^{1}H dipolar couplings obtained from PDLF are compared with off magic angle spinning (OMAS) PDLF. The orientational order is determined from PDLF and ^{13}C-^{1}H dipolar couplings are compared with literature reported values. The remarkable feature of PDLF is the ability to find long range dipolar couplings with better line widths. This enables one to use them for probing the order of phenyl rings where long range couplings for both ortho and meta carbons is common feature. The basic principle of PDLF is to get the proton signal in the dipolar dimension in the presence of multiple pulse homo nuclear dipolar decoupling. This is in contrast to conventional SLF where ^{13}C spectrum is measured in the presence of multiple pulse homo nuclear dipolar decoupling. The PDLF uses MREV-8 multiple pulse for decoupling and the scaling factor is 0.47.

Historically, at about same time, Opella group announced another pulse sequence based on SLF which is aimed at measuring the ^{15}N–^{1}H dipolar couplings from peptides and proteins. The scheme is known as Polarisation Inversion Spin Exchange at the Magic Angle (PISEMA) which uses flip-flop Lee-Goldburg (FFLG) decoupling sequences for suppressing the homo nuclear dipolar interactions [83, 84]. In this, after spin-lock cross polarisation from abundant (I) spins to dilute spins (S), FFLG pulse sequence is used to spin-lock I spins along the magic angle. The high resolution obtained for ^{15}N-acetylleucine is confirmed by comparing the results with conventional SLF scheme. The important feature of PISEMA is high scaling factor (0.82) along with improved resolution of dipolar couplings when compared to conventional SLF. However, it uses FFLG decoupling which is proton offset dependent scheme. When it is extended for liquid crystals for measuring ^{13}C–^{1}H dipolar couplings, optimization of offset for total ^{13}C spectral width is difficult. In other words, if offset is placed in the upfiled region (core units carbons) the down filed region spectral resolution is lost and vice versa. Additionally, RF power used in the SEMA period of PISEMA experiments is high leading to heating of the sample thus changing the measurement temperature. Furthermore, the –CH dipolar couplings found from PISEMA are doublets and the long range couplings noticed in PDLF are no longer available. Despite these limitations, the

PISEMA has found application for measuring the dipolar couplings for liquid crystals mainly due to high scaling factor and better resolution [46, 62]. In a way, the offset problem associated with PISEMA has not mattered much as the orientational order of a liquid crystal is primarily contributed by core unit.

Ramamoorthy's group, in an attempt to address the RF power problem of PISEMA for liquid crystals, modified PISEMA sequence using Time averaged nutation (TAN). The PITANSEMA is based on the PISEMA sequence except change in the t_1 period. PITANSEMA uses unequal durations of flip-flop LG sequences. As a result, effective nutation is scaled by time average factor. The utility of PITANSEMA is initially demonstrated on a dipeptide for ^{15}N–^{1}H dipolar coupling and liquid crystal for ^{13}C–^{1}H dipolar coupling respectively [74]. Later it has been applied to new mesogens for determing the ^{13}C–^{1}H dipolar couplings and computing the orientational order [85]. Though the use of RF power for the PITANSEMA is three times lower than PISEMA, the scaling factor reduced to 0.6 and the line width of dipolar slices are marginally increased.

Ramanathan and co workers, in 1996, demonstrated the utility of cross-polarization based separated local field spectroscopy (CP-SLF) [86]. The approach involves effective use of dipolar oscillations of isolated C–H pair in a liquid crystal molecule during the time of polarization transfer under Hartmann-Hahn condition in CP experiment. Usually, the polarisation transfer between nuclei takes place in a coherent and oscillatory fashion and use of such CP oscillations for measuring dipolar couplings and measuring molecular order in liquid crystals is straightforward. They also suggested a two-dimensional experiment based on the idea of depolarization of rare spins for the determination of oscillation frequencies. The utilty of the scheme is demonstrated by determining the orientational order of MBBA [86].

Very recently, Opella group introduced new pulse scheme termed as SAMPI4 [87]. It uses magic sandwich pulses and as a result the offset dependency of PISEMA problem is addressed. In other words, the SAMPI4 effectively addresses ^{1}H offset issue while retaining the high resolution component of PISEMA. In that sense it is devoid of band width limitations. The utility of SAMPI4 for ^{15}N–^{1}H dipolar couplings is demonstrated for model peptide and membrane proteins. Interestingly, the scaling factor (1.09) is found to be higher than PISEMA (0.82). The utility of SAMPI4 for measuring the ^{13}C–^{1}H dipolar couplings of liquid crystals has been recently reported [88]. The SLF spectra obtained from SAMPI4 of liquid crystals clearly showed high resolution dipolar slices both for the core and terminal units. Moreover, in some cases the ^{13}C–^{1}H dipolar coupling line widths are found to be as low as ∼150 Hz [88].

Applications to liquid crystals

The utility of ^{13}C NMR and SLF for characterization of thermotropic liquid crystals is discussed in this section. Among the mesogens covered (i) 4-hexyloxy benzoic acid (HBA) (T_{C-N}105.4°C–T_{N-I}153.2 ° C), 4'-pentyl-4-biphenylcarbonitrile (5CB) (T_{C-N}24.0°C–T_{N-I}35.3°C), 4-(4-ethoxybenzylidene)-4-butylaniline (EBBA) (T_{C-N} 36.5°C–T_{N-I} 79.8°C) are commercially available while (4-(dodecyloxy)benzoic acid 4-[((4-(di-methylamino)phenyl)imino)methyl]phenyl ester), (DoBDPMP) (T_{C-N} 146.0°C–T_{N-I} 209.3°C), 4-{[thien-3-ylmethylene]amino}phenyl-4-butoxybenzoate (TMAPB) (T_{C-N} 124.0°C–T_{N-I} 153.8°C), 4-{[(thien-3-ylcarboxy) phenyl]-methyleneamino}phenyl-4-tetradecyloxybenzoate (TCPMAPTdB) (T_{C-N} 141.3°C–T_{N-I} 252.3°C) are synthesized in the lab. All of them show enantiotropic nematic phase. The ^{13}C NMR (ID) and SLF spectroscopy are measured while heating the sample in the mesophase. In some nematogens, measurements are carried out at different temperatures. In the case of 1D NMR, the change in chemical shift values is noticed in the nematic phase compared to their respective isotropic values. The alignment of mesogen in the field is indicated by noticing the change in the chemical shift values.

HBA

HBA exhibits nematic phase and the ^{13}C NMR (1D) of the same is shown in Figure 4 along with the molecular structure. Due to the presence of carboxylic group at one terminal, it forms intermolecular hydrogen bonding leading to dimerisation. Earlier studies indicated that the dimeric nature of the HBA is evident both in solid and mesophase [89]. The 1D spectrum shows four lines for the phenyl ring indicating that the two phenyl rings in the dimer are chemically equivalent. Further, two lines for ortho and meta carbons suggest that the phenyl rings are involved in π-flips. The measurements at different temperatures yielded alignment induced chemical shifts which are tabulated in the Table 1. It is clear from the Table 1 that the AIS of para carbons is higher than ortho carbons. This is attributed to close proximity of molecular axis to para carbons than ortho carbons. In other words, the higher principal axis of the shielding tensor (σ_{zz}) of para carbons is parallel to molecular axis. In addition, the chemical environment of para carbons also contributes for higher AIS values. In the case of terminal chain, the chemical shift values of carbons show upfield shift in contrast to phenyl ring and carbonyl carbon and the magnitude of AIS is low. The narrow chemical shift

Figure 4: Molecular structure, ^{13}C NMR spectra and ^{13}C–^{1}H dipolar couplings by SAMPI4 at 119.0°C (a), 128.0°C (b), 138.0°C (c) and (d) 148.0°C of HBA (nematic phase).

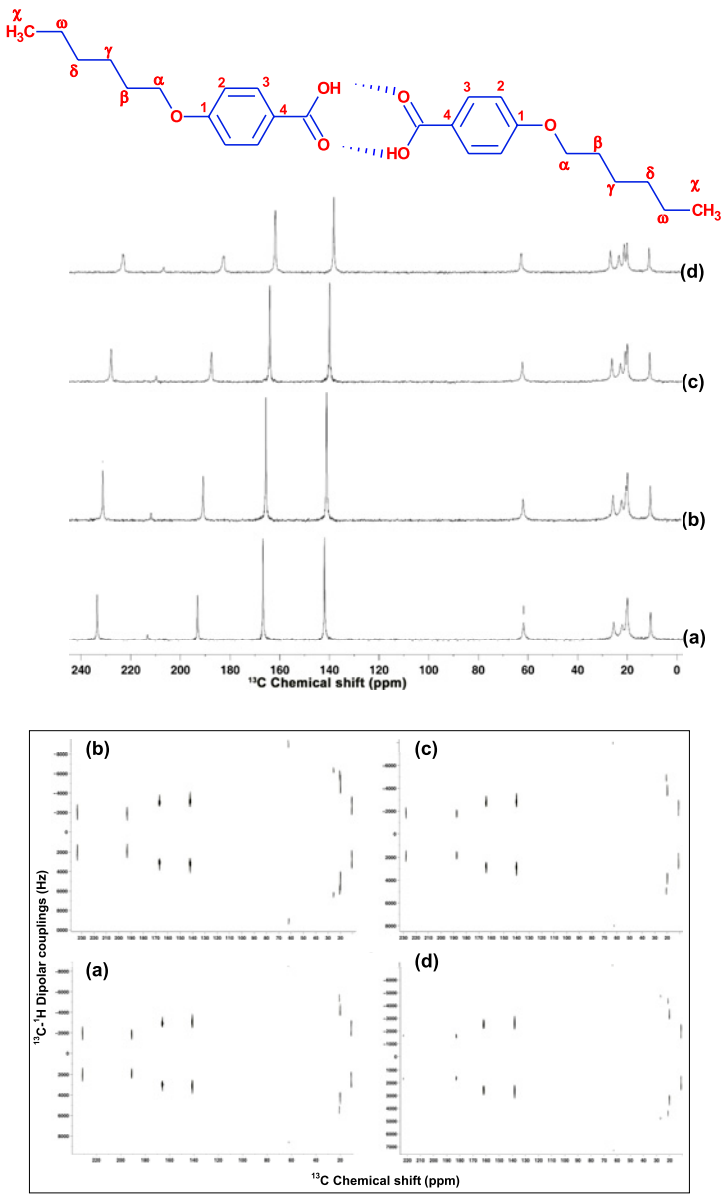

span of aliphatic carbons results in low AIS values in contrast to core unit carbons. These trends support that the molecular axis is parallel to magnetic field axis.

The 2D SLF (SAMPI4) of HBA at different temperatures is shown in Figure 4. The 2D spectra show four contours for the phenyl rings. This further supports the 1D observation where four lines are noticed for two rings (dimer). The ^{13}C–^{1}H dipolar couplings are listed in Table 2. Among the four contours, two are in the range of 2.52–2.62 kHz while the other two showed 1.62 & 1.68 kHz (148.0°C). The higher dipolar couplings are attributed to ortho and meta carbons due to direct couplings while the lower ones are assigned to quaternary carbons that are engaged in long-range couplings. The similar ^{13}C–^{1}H dipolar couplings (5% experimental error) of aromatic methines clearly support that the molecular axis is almost parallel to C2 (para) axis. The same trend is observed at other temperatures also. The ^{13}C–^{1}H dipolar couplings can be used for computing the orientational order parameter using the equation $D = -S(h\gamma_C\gamma_H/4\pi^2 r_{CH}^3)(3\cos^2\theta - 1)/2$ where D is ^{13}C–^{1}H dipolar couplings and θ is angle between C–H vector and magnetic field axis (director) and S is orientational order parameter. The literature reported S value for HBA is 0.61 at 128°C [90]. Using the S value, the θ of C–H vector for two phenyl ring carbons are found to be 118° and 118.3° with respect to director at 128.0°C. By using these θ values and ^{13}C–^{1}H dipolar couplings at other temperatures, the S values are found to be 0.63, 0.56 and 0.52 at 109.0°C, 138.0°C and 148.0°C respectively.

EBBA

EBBA is one of the important nematogens used for studying molecular order by NMR due to its low melting temperature. The molecular structure, 1D and 2D spectra of EBBA are shown in Figure 5. EBBA core consists of two phenyl rings linked by azomethine at para position while one ring has 4 carbon chain and the other has methoxy group. The alignment induced chemical shifts and ^{13}C–^{1}H dipolar couplings are listed in Table 3. In this case too, the quaternary carbons show higher AIS values compared to ortho and meta carbons. The ^{13}C–^{1}H dipolar coupling values are in the range of 2.39–2.60 kHz and small variation in two rings suggests that the molecular axis and C2 axis of respective rings are not collinear and make small angle. The orientational order parameter can be calculated using the ^{13}C–^{1}H dipolar couplings as reported in literature [91].

5CB

5CB is one of the most popular nematogens reported in the literature [92]. The remarkable feature of 5 CB is its mesophase range. It melts to nematic phase at 24.0°C clears at 35.3°C. Additionally, the mesogen is chemically stable in contrast to MBBA or EBBA which are prone to hydrolytic and oxidative degradation on prolonged usage. The molecular structure, 1D and 2D spectra of 5 CB are shown in Figure 6. Similar to EBBA it has two rings in the

Table 1: ^{13}C chemical shifts of HBA and AIS values.

Carbon number	Soluiton chemical shift (ppm) δ_{sol}	Nematic chemical shift (ppm) δ_{lc}(128.0°C)	Alignment induced shift (AIS) (ppm) $(\delta_{lc} - \delta_{sol})$
1	163.7	231.3	67.6
2	114.2	141.0	26.8
3	132.3	165.6	33.3
4	121.4	190.8	69.4
CO	172.2	211.9	39.7
α	68.3	61.9	–6.4
β	29.1	22.2	–6.9
γ	25.6	22.0	–3.6
δ	31.5	25.6	–5.9
ω	22.6	19.8	–2.8
χ	14.0	10.6	–3.4

core but is directly linked without any connecting unit. One ring has polar cyano group as terminal group while the other ring has pentyl chain. The ^{13}C–^{1}H dipolar couplings of the nematogen along with chemical shift values are listed in Table 4. The ^{13}C–^{1}H dipolar couplings are in the range of 1.91–2.15 kHz and the orientational order parameter (S) reported in the literature is typically 0.51 [93].

DoBDPMP

DoBDPMP is a nematogen synthesized in the lab as reported in literature [94]. It consists of three phenyl rings linked by ester and azomethine connecting units with alkoxy chain at one end and dimethylamino group at other termini. As a result, the nematogen melts at 146.0°C and clears at 209.3°C. Additionally, it also exhibits smectic A phase at 107.1°C monotropically. The nematogen assumes importance in view of dimethylamino group which act as charge-transfer donor. Figure 4 & 5 show the molecular structure, 1D and 2D spectrum of DoBDPMP. The ^{13}C NMR in solution, CP-MAS in solid state and static spectrum (155.0°C) in the nematic phase are shown in Figure 7 while Figure 8 depicts the 1D and ^{13}C–^{1}H dipolar coupling spectra of DoBDPMP determined by PITANSEMA at different temperatures. The high resolution nature of the spectrum in solution indicates fast molecular tumbling of the mesogen while the relatively broad lines in CP-MAS spectrum

Figure 5: EBBA molecular structure, ^{13}C NMR spectrum and ^{13}C–^{1}H dipolar couplings by SAMPI4 at 45.0°C (nematic phase).

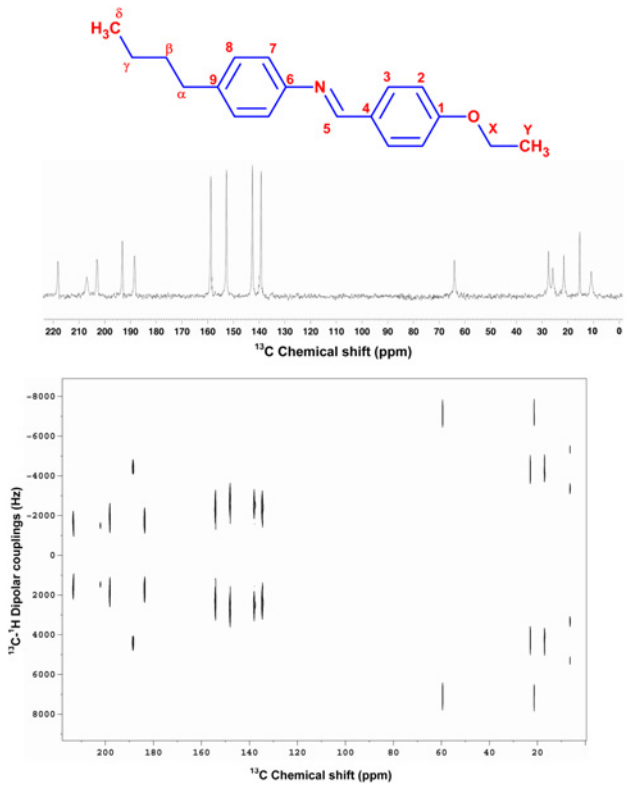

Table 2: ^{13}C chemical shifts and ^{13}C–^{1}H Dipolar couplings of HBA at different temperatures measured by SAMPI4.

Carbon No	Chemical shift 148.0°C	Dipolar couplings (kHz) 148.0°C	Chemical shift 138.0°C	Dipolar couplings (kHz) 138.0°C	Chemical shift 128.0°C	Dipolar couplings (kHz) 128.0°C	Chemical shift 119.0°C	Dipolar couplings (kHz) 119.0°C
1	223.1	1.68	227.9	1.88	231.3	1.89	233.5	1.95
2	138.0	2.61	139.8	2.86	141.0	3.03	141.9	3.13
3	161.6	2.52	163.9	2.75	165.6	2.92	166.7	3.03
4	182.6	1.62	187.5	1.79	190.8	1.85	193.1	1.91

Table 3: ^{13}C chemical shifts, AIS and ^{13}C–^{1}H Dipolar couplings of EBBA measured by SAMPI4 (only core unit carbons are shown).

Carbon number	Soluiton chemical shift (ppm) δ_{sol}	Nematic phase Chemical shift (ppm) (δ_{lc}) 45.0°C	Alignment induced shift (AIS) (ppm) ($\delta_{lc} - \delta_{sol}$)	^{13}C–^{1}H dipolar couplings (kHz) 45.0°C
4	130.2	188.4	58.2	1.64
5	158.6	193.1	34.5	4.38
9	140.1	202.9	62.8	1.98
6	149.8	206.9	57.1	1.46
1	161.3	218.1	56.8	1.69
2	129.1	158.7	29.6	2.39
8	128.9	152.6	23.7	2.60
7	120.6	142.5	21.9	2.51
3	114.4	139.2	24.8	2.41

Table 4: ^{13}C chemical shifts and ^{13}C–^{1}H Dipolar couplings of 5CB measured by SAMPI4 (only core unit carbons are shown).

Carbon number	Solution chemical shift (ppm) δ_{sol}	Nematic chemical shift (ppm) (δ_{lc}) 22.0°C	Alignment induced shift (AIS) (ppm) ($\delta_{lc} - \delta_{sol}$)	^{13}C–^{1}H dipolar couplings (kHz) 22.0°C
4	145.6	195.2	49.6	1.73
1	110.6	194.2	83.6	1.22
8	143.9	183.8	39.9	1.27
5	136.4	164.8	28.4	1.24
2	132.6	154.0	21.4	1.91
7	129.3	145.4	16.1	2.12
3	127.5	143.3	15.8	2.08
6	127.1	141.4	14.3	2.15

suggest the molecular rotations are frozen. The static spectrum in nematic phase, in contrast to CP-MAS, shows well resolved sharp lines clearly indicating the alignment of the mesogen in the magnetic field (Figure 7 & Table 5). The assignment of static spectral lines is attempted by comparing with that of HBA which is structurally similar to the starting material of the mesogen. Accordingly, the ring 1 assignment of four carbons is done by considering the HBA ^{13}C chemical shifts. The influence of temperature on AIS and ^{13}C–^{1}H dipolar couplings is evident from Figure 8 (Table 6). As the temperature is increased in nematic phase, the molecules undergo fast rotations and eventually onset of molecular tumbling is noticed. The orientational order parameter (S) is calculated from the ^{13}C–^{1}H dipolar couplings of azomethine which are found to be 0.63–0.45 in the temperature of 155.0–200.0°C [95]. The close examination of ^{13}C–^{1}H dipolar couplings at any given temperature indicates that

Figure 6: Molecular structure of 5CB, ^{13}C NMR spectrum and SAMPI4 in the nematic phase (23.0°C).

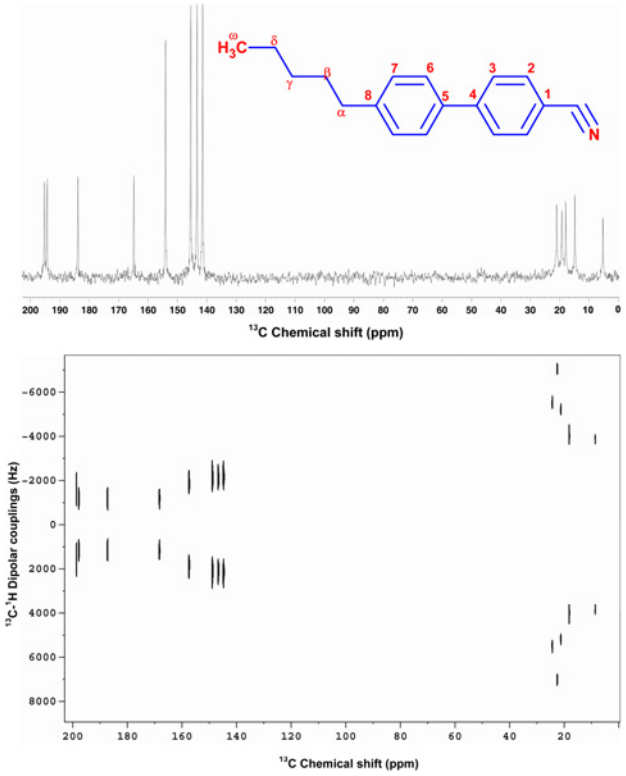

Figure 7: ^{13}C solution (A), ^{13}C CP-MAS (B) and static ^{13}C NMR (C) spectra of DoBDPMP (155.0°C) in nematic phase along with molecular structure.

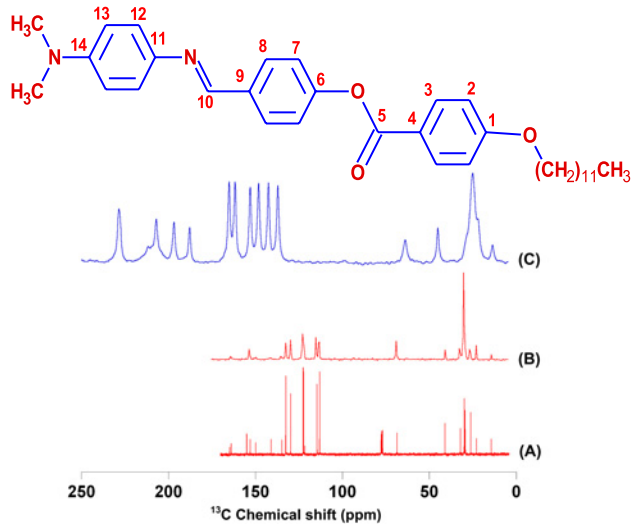

Table 5: ^{13}C chemical shifts and AIS of DoBDPMP (only core unit carbons are shown).

Carbon number	Solution chemical shift (ppm) δ_{sol}	Nematic phase (ppm) 150.0°C (δ_{lc})	AIS (ppm) 150.0°C ($\delta_{lc} - \delta_{sol}$)
5	164.6	228.4	63.8
1	163.6	228.4	64.8
10	154.7	196.8	42.1
14	152.8	208.1	55.3
6	149.5	211.6	62.1
11	140.7	206.9	66.2
9	134.4	187.7	53.3
8	132.3	165.1	32.8
3	129.4	161.7	32.3
7	122.2	152.9	30.7
12	122	148.1	26.1
4	121.3	187.7	66.4
2	114.3	142.5	28.2
13	112.8	137.1	24.3

Table 6: AIS of DoBDPMP measured by static ^{13}C NMR at different temperatures.

Carbon number	AIS (ppm) 155.0°C	^{13}C–^{1}H dipolar couplings (kHz) 155.0°C	AIS (ppm) 170.0°C	^{13}C–^{1}H dipolar couplings (kHz) 170.0°C	AIS (ppm) 185.0°C	^{13}C–^{1}H dipolar couplings (kHz) 185.0°C	AIS (ppm) 200.0°C	^{13}C–^{1}H dipolar couplings (kHz) 200.0°C
2	27.3	3.29	25.8	3.16	23.6	2.81	20.3	2.37
12	25.7	2.53	24.4	2.38	22.5	2.21	19.6	1.83
7	29.9	2.79	28.3	2.73	25.9	2.50	22.1	2.01
13	23.6	2.43	22.6	2.28	21.0	2.13	18.5	1.86
3	31.9	2.60	30.4	2.50	27.9	2.25	24.1	1.85
8	32.5	2.40	30.6	2.30	27.8	2.08	23.7	1.76
10	42.0	4.66	39.8	4.33	36.4	4.00	33.5	3.35
14	55.2	–	53.7	–	49.2	–	42.9	–
11	66.2	–	62.5	–	56.9	–	53.6	–
9	53.3	–	50.0	–	44.6	–	36.3	–
6	62.0	–	58.9	–	53.6	–	48.3	–
5	63.8	–	60.0	–	54.2	–	46.1	–
1	64.8	–	61.0	–	55.2	–	47.2	–

the molecular axis and C2 axes of any phenyl rings make a small angle of tilt.

TMAPB

TMAPB is a thiophene containing nematogen. It melts at 124.0°C to nematic phase and clears at 153.8°C [96]. Thiophene, in recent decade, has attracted the attention of many synthetic and material chemists due to its versatile nature [96]. The five member geometry, aromatic character, ability to undergo many chemical transformations at 2 & 3 positions, charge transfer donating and accepting features, conducting/semiconducting ability etc., are some of the remarkable features of thiophene. It is found in liquid crystal research that the insertion of thiophene in the mesogens consisting of phenyl rings, would contribute to an increase of optical anisotropy, a decrease of the melting point, a promotion of a negative dielectric anisotropy, a reduction in viscosity, and fast switching times [97]. As a consequence, many research studies have been undertaken by different groups for exploring properties like conducting plastics, plastic electronics, light emitting liquid crystals, thin film transistors, light emitting diodes, solar cells etc. [96] In an attempt to understand the role of thiophene geometry on the liquid crystalline property, first time, solid state ^{13}C NMR spectroscopy is used [97].

The molecular structure, static ^{13}C NMR and 2D (PITANSEMA) of TMAPB is shown in Figure 9.

Table 7: ^{13}C chemical shifts, AIS and ^{13}C–^{1}H Dipolar couplings of TMAPB measured by PITANSEMA (only core unit carbons are shown).

Carbon number	Soluiton chemical shift (ppm) (δ_{sol})	Nematic Chemical shift (ppm) 130.0°C (δ_{lc})	Alignment induced shift (AIS) (ppm) ($\delta_{lc} - \delta_{sol}$)	^{13}C–^{1}H Dipolar couplings (kHz) 130.0°C
1	163.6	221.7	58.1	–
2	114.3	138.5	24.2	2.25
3	132.3	161.4	29.1	2.20
4	121.6	181.5	59.9	–
5	165.0	215.8	50.8	–
6	149.2	193.4	44.2	–
7	121.7	144.4	17.3	2.40
8	122.4	149.5	27.1	2.20
9	149.6	205.6	56.0	–
10	154.5	194.1	39.6	4.25
11	140.8	176.4	35.6	–
12	130.3	150.0	19.7	5.50
13	126.0	138.0	12.0	3.60
14	126.7	139.2	12.5	4.40

Table 8: ^{13}C chemical shifts, AIS and ^{13}C–^{1}H Dipolar couplings of TCPMAPTdB measured by PITANSEMA (only core unit carbons are shown).

Carbon number	Solution chemical shift (ppm) δ_{sol}	Nematic chemical shift (ppm) 150.0°C δ_{lc}	Alignment induced shift (AIS) (ppm) ($\delta_{lc} - \delta_{sol}$)	^{13}C–^{1}H Dipolar couplings (kHz) 150.0°C
5	164.1	217.2	53.1	–
1	162.7	231.3	68.6	–
15	162.2	233.3	71.1	–
10	160.4	204.8	44.4	5.20
14	155.4	229.1	73.7	–
6	150.1	210.7	60.6	–
9	150.0	210.7	60.7	–
11	134.0	192.1	58.1	–
12	134.1	167.0	32.9	2.80
17	131.9	162.4	30.5	4.86
3	131.1	164.2	33.1	3.01
16	131.0	176.0	45.0	–
18	129.0	152.8	23.8	6.48
19	125.4	144.5	19.1	5.00
13	124.8	149.5	24.7	3.23
8	122.8	155.0	32.2	2.90
4	122.4	176.0	53.6	–
7	121.9	154.3	32.4	2.90
2	114.2	143.8	29.6	2.98

The mesogen consists of two phenyl rings linked by ester group while the thiophene is connected by azomethine at 3-posiiton. The alignment of the mesogen in the magnetic field is noticed by change in the chemical shifts. The AIS values of the nematogen at 130.0°C are listed in Table 7. It is clear from the spectrum that the thiophene methine ^{13}C chemical shifts and phenyl ring methine ^{13}C chemical shifts are overlapping as both of them are aromatic and experiencing similar chemical environment. The quaternary carbons of both thiophene and phenyl rings, on the other

Figure 8: 1D and 2D (PITNASEMA) spectra of DoBDPMP at 155.0 (a), 170.0 (b), 185.0 (c) and 200.0°C (d).

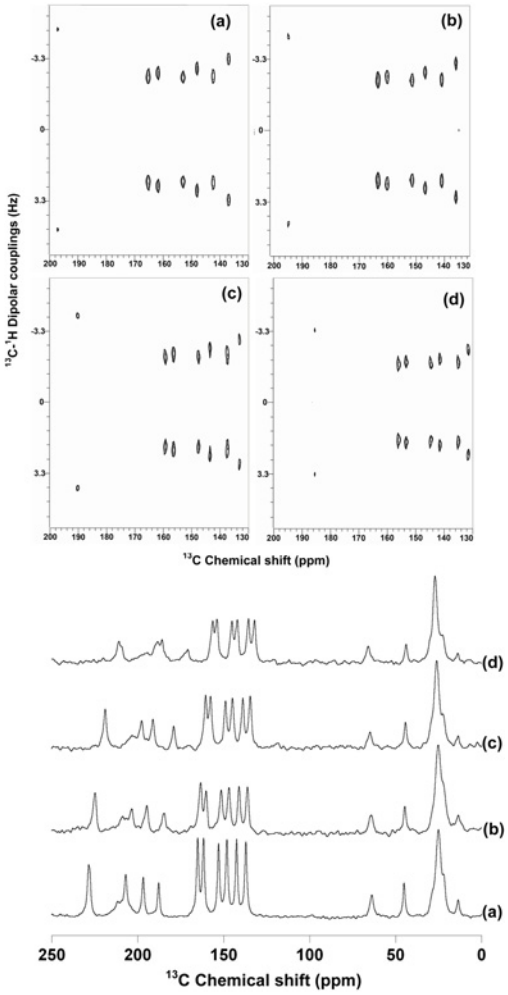

Figure 9: TMAPB molecular structure, ^{13}C NMR spectrum and ^{13}C–^{1}H dipolar couplings by PITANSEMA at 130.0°C (nematic phase).

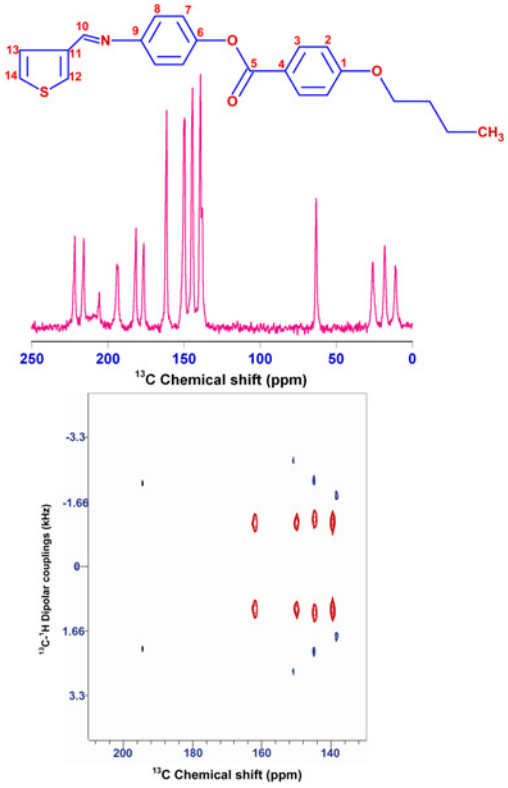

hand, show better resolution. Figure 9 shows the 2D (PITANSEMA) of TMAPB at 130.0°C. The remarkable feature of the spectrum is clear separation of phenyl ring methines (red contours) from thiophene methines (blue contours). The separation of C–H vectors for thiophene and phenyl which is not possible with 1D data mainly arises due to orientation of molecular axis in the magnetic field. In other words, the methines of thiophene are experiencing different geometrical environment in contrast to phenyl ring methines. This is attributed to hexagonal geometry of phenyl ring and the irregular pentagon of thiophene. As a result, the thiophene C–H vectors showed higher magnitude than phenyls though the chemical shifts are comparable. This particular study clearly demonstrates the power of 2D solid state ^{13}C NMR for probing mesogens which are different from conventional mesogens.

By using the ^{13}C–^{1}H dipolar couplings of azomethine, the orientational order for TMAPB is calculated which is found to be 0.60 [97]. Since the CSA values of thiophene are not available in the literature, the AIS values of thiophene unit could not be assigned precisely. Similarly, the geometrical information of thiophene ring in the mesophase is also not available thus making it difficult to determine the order parameter of thiophene unit. However, the projection of three C–H vectors of thiophene are calculated using the order parameter value of core (0.6) with respect to molecular axis and are found to be in range of 37–43° [97].

TCPMAPTdB

To verify and confirm the interesting features observed for TMAPB in nematic phase, solid state ^{13}C NMR spectroscopy of TCPMAPTdB which is also thiophene based is undertaken. TCPMAPTdB is also a nematogen and consists of three phenyl rings linked by ester and azomethine and connected

Figure 10: TCPMAPTdB molecular structure, ^{13}C NMR spectrum and ^{13}C–^{1}H dipolar couplings by PITANSEMA at 150.0°C (nematic phase).

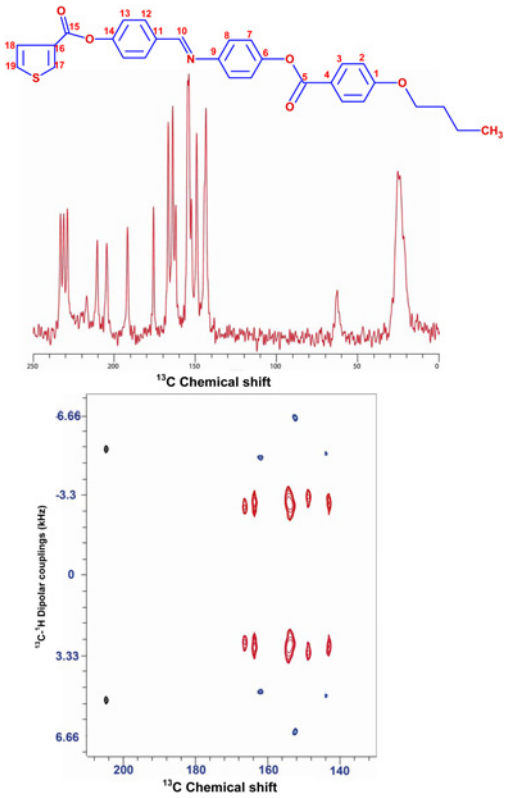

to thiophene at one terminal by ester group [98]. It melts at 141.3°C to nematic phase and clears at 252.3°C. The molecular structure, 1D and 2D spectra measured at 150.0°C are shown in Figure 10. The AIS values support the parallel alignment of the mesogen in the magnetic field (Table 8). In this case too, the 1D spectrum shows overlap of some of the thiophene signals with phenyl ring methines. Like earlier case (TMAPB), the 2D NMR spectrum clearly resolves them because of different geometry and orientation of the thiophene ring compared to that of phenyl ring. However, the pattern observed for thiophene CH's (blue contours) is slightly different from those of TMAPB suggesting that the thiophene in TCPMAPTdB experiences different geometrical environment. The ^{13}C–^{1}H dipolar couplings as listed in the Table 8 support the inference.

Future role of solid state ^{13}C NMR

The examples cited in the article are calamitic nematogens and are structurally simple systems. However, to probe structurally complex mesogens reported in recent literature [14, 18, 99], by solid state ^{13}C NMR is a real challenge. Additionally, investigating the role played by alkyl/alkoxy chain in terms of length, position and chemical nature in imparting nano-segregation leading to complex mesophase morphologies of mesogens has not been attempted by solid-state ^{13}C NMR. It demands not only 1D and 2D techniques, but also invoking complex relaxation mechanisms. The determination of CSA of different carbons of functionalities involved in the liquid crystal research would be of use for examining the AIS values. Furthermore, study of non-linear mesogens (un-conventional mesogens) should be possible by solid state ^{13}C NMR. Specifically, the ^{13}C–^{1}H dipolar couplings of core can precisely provide information about location of molecular axis thus paving the way for establishing the topology. In other words, linear, hockey-stick, bent-core, lamda, S-shape, H-Shape, T-shape, star and other molecular architectures [99,100] in principle can be investigated by solid-state ^{13}C NMR spectroscopy. It is hoped that the coming decade would witness routine use of ^{13}C NMR for structural and geometrical investigations of mesogens in the mesophase.

Conclusion

In this article an attempt is made to explain and highlight the salient features of solid-state ^{13}C NMR spectroscopy and its application to thermotropic liquid crystals. The utility and significance of natural abundance ^{13}C over deuterium NMR is addressed. The importance of alignment induced chemical shifts from 1D and ^{13}C–^{1}H dipolar couplings from 2D experiments for understanding the molecular structure and organization in the mesophase is briefly described. The developments that have taken place since the introduction of ^{13}C NMR and separated local field spectroscopy for liquid crystals is covered. The utility of each new pulse sequence from the conventional SLF to SAMPI4 are mentioned including the importance of different homo-nuclear decoupling sequences. The role of molecular axis, its alignment in the magnetic field and its influence on chemical shift values is explained. The power of 1D and 2D ^{13}C NMR spectroscopy to (mostly) nematogens including newly synthesized are described. The remarkable feature of 2D over 1D solid-state ^{13}C NMR spectroscopy is demonstrated for the case of thiophene nematogens. The specific advantage of ^{13}C NMR spectroscopy for mesogens consisting other than hexagonal geometry is explicit as noticed for thiophene mesogens. The utility of ^{13}C–^{1}H dipolar couplings for computing the orientational order (S) is briefly discussed for the case of HBA. The possible future role of solid state ^{13}C NMR spectroscopy for structurally complicated mesogens and understanding their self organization is briefly mentioned.

Acknowledgments

The author would like to sincerely thank Dr. A. B. Mandal, Director, CLRI for his support. The interest and encouragement of Dr. N. Somanathan and other polymer lab colleagues in this work is duly acknowledged. He also would like to place on record the support and collaboration of Prof. K. V. Ramanathan, Chairman, NMR Research Center, IISc, Bangalore for solid state ^{13}C NMR work. Mr. Bibhuti Das and Mr. Nitin Lobo, IISc, Bangalore are thanked for some of the 1D and 2D spectra. The partial financial support from NWP-23 is gratefully acknowledged. Dr. T. Ramasami, Secretary, DST, India and former Director, CLRI is thanked for his support at the initial stage of advanced materials research. Finally thanks are due to Prof. A. Ramamoorthy, Department of Chemisrty, University of Michigan, Ann Arbor for the initiation of ^{13}C NMR liquid crystal work during authors sabbatical stay in his lab.

Received 19 October 2009; accepted 16 January 2010.

References

1. C. N. R. Rao, *University General Chemistry: An Introduction to Chemical Science*, MacMillan India, 2000, New Delhi.
2. P. Atkins and J. D. Paula, *Physical Chemistry*, Oxford University Press, 2006. London.
3. R. G. Mortimer, *Physical Chemsitry*, Academic Press, 2000, San Diego.
4. F. D. Saeva, *Liquid Crystals: The Fourth State of Matter*, 1979, Marcel Dekker, New York.
5. N. V. Madhusudana, *Current Science*, 80, 25 (2001).
6. B. Donnio and D.W.Bruce, *Struct. Bond.,* 95, 193 (1999).
7. E Reinitzer, *Monatsh. Chem.* 9, 421 (1888); English version *Liq. Cryst.,* 5, 7 (1989).
8. O. Lehmann, *Z. Phys. Chem.,* 4, 462 (1889); D. Vorlander and F. Meyer, Liebigs, *Ann. Chem.* 320, 122 (1902); G. Friedel. *Ann. Physique* 18, 273 (1922); V. Vill, *Mol. Cryst. Liq. Cryst.* 213, 67 (1992).
9. P. Oswald and P. Pieranski, *Nematic and Cholesteric Liquid Crystals*, CRC Press, Taylor & Francis, 2005, London.
10. W. Helfrich and M. Schadt, *Swiss Patent CH 532 261*,1970, Zurich.
11. S. Chandrasekhar, *Liquid Crystals*, Cambridge University Press, 1994, Cambridge.
12. J. W. Goodby, D. W. Bruce, M. Hird, C. Imrie and M. Neal, *J. Mater. Chem.,* 11, 2631 (2001).
13. D. Pauluth and K. Tarumi, *J. Mater. Chem.,* 14, 1219 (2004).
14. J. W. Goodby, *Chem. Soc. Rev.,* 36, 1855 (2007).
15. S. Sergeyev, W. Pisulab and Y. H. Geerts, *Chem. Soc. Rev.,* 36, 1902 (2007); J. Etxebarria and M. Blanca Ros, *J. Mater. Chem.,* 18, 2919 (2008)
16. G. W., Gray, *Molecular Structure and Properties of Liquid Crystals*, Academic Press, 1962. New York
17. J. W. Goodby, I. M. Saez, S. J. Cowling, J. S. Gasowska, R. A. MacDonald, S. Sia, P. Watson, K. J. Toyne, M. Hird, R. A. Lewis, S-E Leec and V. Vaschenko, *Liq. Cryst.,* 36, 567 (2009).
18. C. Tschierske, *Chem. Soc. Rev*., 36, 1930. (2007).
19. D. Janietz and A. Kohlmeier, *Liq. Cryst.,* 36, 685 (2009).
20. C. Tschierske, *J. Mater. Chem*., 11, 2647 (2001).
21. C. Tschierske, *J. Mater. Chem*., 8, 1485 (1998).
22. A. Jakli and A. Saupe, *One- and Two-Dimensional Fluids: Properties of Smectic, Lamellar and Columnar Liquid Crystals,* Taylor & Francis, 2006, London.
23. I. Dierking, *Texture of Liquid Crystals*, Wiley VCH, 2003, Weinhiem.
24. *Solid-State NMR Spectroscopy: Principles and Applications*, Ed., M.J.Duer, Blackwell, 2002, London.
25. *Optical Applications of Liquid Crystals,* Ed., L Vicari, IOP Publishing, 2003, London.
26. *Handbook of Liquid Crystals*, Vol. 1, Ed., D. Demus, J. W. Goodby, G. W. Gray H.-W. Spiess and V., Vill, Wiley-VCH, 1998, Weinheim,.
27. R. W. Lenz, *Pure Appl.Chem.,* 57, 977 (1985).
28. T. Perova, A.Kocot and J. K. Vij , *Mol. Cryst. Liq. Cryst., 301,* 111, (1997).
29. F. Beekmans and P. D. Boer, *Macromolecules* 29, 8726(1996); E. Chrzumnicka, M. Szybowicz and D. Bauman, Z. *Naturforsch., A: Phys. Sci*., 59, 510 (2004); M. C. W. Van Boxtel, M. Wubbenhorst, J. Vanturnhout, C. W. M. Bastiaansen and D.J. Broer, *Liq. Cryst.* 30, 235 (2003); J. K. Vij, A. Kocot, T. S. Perova, *Mol. Cryst. Liq. Cryst.,* 397, 231/[531] (2003).
30. A. J. Seed, K. Toyne, J.W. Goodby and M. Hird, *J. Mater. Chem*. 5, 1 (1995).
31. T. D. W. Claridge, *High-Resolution NMR Techniques in Organic Chemistry*, Tetrahedron Organic Chemistry series, 27, Elesevier, 2009, Oxford.
32. K. V. Ramanathan and Neeraj Sinha, *Monatshefte fur Chemie*.,133,1535 (2002); V. Domenici, M. Geppi and C. A. Veracini, *Progress in NMR*, 50 1 (2007).
33. A. Saupe and G. Englert, *Phys. Rev. Lett.,* 11, 462 (1963).
34. P. Jain, H. A. Moses, J. C. Lee and R. D. Spence, *Phys. Rev,* 92, 844 (1953); H.Lippmann, *Ann. Physik.,* 2, 281 (1958); K. H.Weber, *Ann, Physik,* 3, 1 (1959).
35. *Nuclear Magnetic Resonance of Liquid Crystals*, Emsley J. W. (Ed.) Reidel, 1985, Dordrech; *Encyclopedia of NMR*, Dong RY, DM Grant and Harris RK, (Eds) Wiley, 1996, Chichester; R. Y. Dong, *Prog Nucl Magn Reson Spectrosc* 41,115 (2002).
36. V. Domenici, *Pure Appl. Chem.,* 79, 21 (2007).
37. A. Ramamoorthy, Ed., *Thermotropic Liquid Crystals: Recent Advances*, Springer, 2007, Dordrecht, The Netherlands.
38. S. V. Dvinskikh, Z. Luz, H. Zimmermann, A. Maliniak and D. Sandstrom, *J. Phys. Chem. B*. 107, 1969 (2003); S. V. Dvinskikh, K. Yamamoto, D. Scanu, R. Deschenaux, and A. Ramamoorthy, *J. Phys. Chem. B.*, 112, 12347 (2008); M. Geppi, A. Marini, C. A. Veracini, S. Urban, J. Czub, W. Kuczynski and R. Dabrowski, *J. Phys. Chem. B*. 2008, 112, 9663.
39. M. H. Levitt, *Spin Dynamics; Basics of Nuclear Magnetic Resonance*, John Wiley, 2008, Chichester.
40. B. M. Fung, *Prog. Nucl. Magn. Reson. Spectrosc.,* 41, 271 (2002).
41. *NMR of Ordered Liquids*, E. E. Burnell and C.A. de Lange (Eds)., Kluwer Academic Publsihers, 2003, The Netherlands.
42. V. Domenici, M. Geppi and C. A. Veracin, *Prog in NMR*, 50, 1 (2007).
43. J. Courtieu, J.P. Bayle and B.M. Fung, *Prog. Nucl. Magn. Reson. Spectrosc.* 26, 141 (1994).
44. T. Nakai, H. Fujimora, D. Kuwari and S. Miyajima, *J. Phys. Chem. B*, 103 417. (1999).
45. W. S. Veeman, *Prog. Nucl. Magn. Reson. Spectrosc.*, 16, 193 (1984).
46. J. Xu, K. Fodor-Csorba and R. Y. Dong, *J. Phys. Chem. A*. 109, 1998 (2005).
47. J. Herzfeld and A. E. Berger, *J. Chem.* Phys. 73, 602l (1980).
48. Z. Gan, *J. Am. Chem. Soc.* 114, 8307 (1992).
49. A. C. Kolbert and R. G. Griffin, *Chem. Phys. Lett.* 166, 87 (1990).
50. S-F. Liu, J-D. Mao and K. Schmidt-Rohr, *J. Magn. Reson.,* 155, 15 (2002).
51. B. Das, S. Grande, W. Weissflog, A. Eremin, M. W. Schroder, G. Pelzl, S. Diele and H. Kresse, *Liq. Cryst.*, 30, 529 (2003).
52. P. J. Collings and M. Hird, *Introduction to Liquid crystals Chemistry and Physics,* Taylor and Francis, 1997, London.

53. A. Pines and J. J.Chang, *Phy. Rev. A* 10, 946 (1974).
54. A. Pines, D. J. Ruben and S. Allison, *Phys. Rev. Lett.,* 17, 1002 (1974)
55. A. Pines and J. J. Chang, *J. Am. Chem. Soc.,* 96, 5590 (1974).
56. A. Pines, *REPORT LBL-4505; CONF-750873-1, 1975,* 55 p., Energy Citation Database.
57. B. M. Fung, *Nuclear Magnetic Resonance Spectroscopy of Liquid Crystals,* Ed., R. Y. Dong, World Scientific, 2009, New Jersey.
58. B. M. Fung and J. Afzal, *J. Am.Chem.Soc.,* 108, 1107 (1986).
59. C. Tan and B. M. Fung, *J. Phys. Chem. B,* 107, 5787 (2003).
60. W. Guo and B. M. Fung, *J. Chem. Phys.,* 95, 3917 (1991).
61. V. Domenici, C. Alberto Veracini, V. Novotn and R. Y. Dong, *Chem Phys Chem.,* 9, 556 (2008); R. Y. Dong, *J. Phys. Chem. B* 113, 1933 (2009); Ronald Y. Dong, J. Xu, J. Zhang and C. A. Veracini, *Phy. Rev. E* 72, 061701 (2005).
62. S. V. Dvinskikh, H. Zimmermann, A. Maliniak and D. Sandstrom, *J. Magn. Res.,* 163, 46 (2003); S. V. Dvinskikh, D. Sandstrom, H. Zimmermann and A. Maliniak, *Prog. Nucl. Magn. Reson. Spectrosc.* 48, 85 (2006).
63. H. Zimmermann, V. Bader, R. Poupko, E. J. Wachtel and Z. Luz, *J. Am. Chem. Soc.,* 2002, 124, 15286.
64. R. Y. Dong, J. Xu, J. Zhang, and C. A. Veracini, Phy. Rev. E., 72, 061701 (2005).
65. S. J. Opella and F. M. Marassi, *Chem. Rev.* 104, 3587 (2004).
66. J. W. Hennel and J. Klinowski, *Top. Curr. Chem.* 246, 1 (2004).
67. J. Schaefer, and E. O. Stejskal, *J. Am. Chem. Soc.* 98, 1031 (1976).
68. M., Mehring, *High Resolution NMR Spectroscopy in Solids*, Springer-Verlag, 1983, New York.
69. R. K. Hester, J. L. Ackerman, B. L. Neff and J. S. Waugh, *Phys. Rev. Lett.,* 36, 1081 (1976).
70. S. Hartmann and E. L. Hahn, *Phys. Rev.,* 128, 2042 (1962).
71. J. S. Waugh, *Proc. Natn. Acad. Sci., USA,* 13, 1394 (1976).
72. S. J. Opella and J. S. Waugh, *J. Chem. Phys.,* 66, 4919 (1977).
73. A. Hohner, L. Muller and R. R. Ernst, *Mol. Phys.,* 38, 909 (1979).
74. A. Ramamoorthy, Y. Wei and D. K. Lee *Annu. Rep. NMR Spectrosc., 52*, 1 (2004).
75. Z. Gan, *J. Magn. Reson.,* 143, 136 (2000).
76. *Encyclopedia of Nuclear Magnetic Resonance,* B. M. Fung, D. M. Grant, R. K. Harris (Eds.), Wiley, 1996, Chichester.
77. F. L.Perez, P. Judeinstein, J. P. Bayle, H. Allouchi, M. Cotrait, F. Roussel and B. M. Fung, *Liq. Cryst.,* 24, 627 (1998).
78. C. D. Poon and B. M. Fung, *Liq. Cryst.,* 5, 1159 (1989).
79. T. H. Tong and B. M. Fung, *Mol. Crys. Liq. Crys.,* 303, 127 (1997)
80. J. P. Bayle and B. M. Fung, *Liq. Cryst.,* 15, 87 (1993).
81. C. Canlet and B. M. Fung *J. Phys. Chem.*, B, 104, 6181 (2000).
82. S. Caldarelli, M. Hong, L. Emsley and A. Pines, *J. Phys. Chem.* 100, 18696 (1996).
83. C. H. Wu, A. Ramamoorthy and S. J. Opella, *J. Magn. Reson. A* 109, 270 (1994).
84. A. Ramamoorthy, C. H. Wu and S. J. Opella, *J. Magn. Reson. B* 107, 88 (1995).
85. D. K. Lee, T.Narasimhaswamy and A. Ramamoorthy, *Chem Phys. Lett.,* 399, 359 (2004).
86. R. Pratima and K. V. Ramanathan, *J. Magn. Reson.*, A 118, 7 (1996).
87. A. A. Nevzorov and S. J. Opella, *J. Magn. Reson.*, 2007, 185, 59.
88. B. B. Das, N. Sinha and K. V. Ramanathan, *J. Magn. Reson.*, 194, 237 (2008)
89. J. C. Rowell, W. D. Philips, L. R. Melby and M. Panar, *J. Chem. Phys.,* 43, 3442 (1965).
90. *Physical Properties of Liquid Crystals, Vol. VIII/5A*, Landolt-Bornstein. Numerical Data and Functional Relationships in Science and Technology. New Series, Ed., S. M. Pestov, Springer, Berlin, 2003.
91. C. S. Nagaraja and K. V. Ramanathan, *Liq. Cryst.,* 26, 17 (1999).
92. Liquid crystals, I-C. Khoo, John Wiley, 2007, New Jeresy.
93. B. M. Fung, J. Afzal, T. L. Foss and M-H. Chau, *J. Chem. Phys* 85, 4808 (1986).
94. T. Narasimhaswamy and K. S. V. Srinivasan, *Liq. Cryst.* 31, 1457 (2004).
95. T. Narasimhaswamy, M. Monette, D. K. Lee and A. Ramamoorthy, *J. Phys. Chem. B*. 109, 19696 (2005).
96. T. Narasimhaswamy, N. Somanathan, D. K. Lee and A. Ramamoorthy, *Chem. Mater. 17*, 2013 (2005); *Functional Organic Materials-Syntheses, Strategies and Applications,* (Eds.), T. J. J. Muller and U. H. F. Bunz, Wiley-VCH Verlag, 2007, Weinheim.
97. N. L. Campbell, W. L. Duffy, G. I. Thomas, J. H. Wild, S. M. Kelly, K. Bartle, M. O'Neill, V. Minter and R. P Tuffin,. *J. Mater. Chem.* 12, 2706. (2002); T. Narasimhaswamy, D. K. Lee, K. Yamamoto, N. Somanathan and A. Ramamoorthy, *J. Am. Chem. Soc. 127*, 6958 (2005);
98. T. Narasimhaswamy, D. K. Lee, N. Somanathan and A. Ramamoorthy, *Chem. Mater. 17*, 4567 (2005).
99. T. Kato, N. Mizoshita and K. Kishimoto, *Angew. Chem.,118*, 44 (2006).
100. I. M. Saez and J. W. Goodby, *Struct. Bond.,* 128, 1 (2008); D.W . Bruce, J. W. Goodby, J. R. Sambles and H. J. Coles, *Phil. Trans. R. Soc. A*, 364, 2567 (2006).

Dr. T. Narasimhaswamy after completing M.Sc., Organic Chemistry from S. K. University, Anantapur, qualified CSIR JRF test and joined as a Research fellow in Central Leather Research Institute, Chennai in 1986. He was awarded Ph.D from University of Madras in the year 1990 for the work on "Phenyl acrylate polymers". He continued in CLRI as Research associate and later joined as a Scientist in Polymer Lab. His areas of research include Synthesis and characterization of thermotropic liquid crystals, Functional monomers and polymers and NMR characterization of soft materials. He was a visiting fellow, University of Michigan, Ann Arbor on sabbatical for a year. He has published 30 research papers in peer reviewed journals and participated in many conferences. His current research focus is on Mesogens, Molecular Topology and NMR.